ESC European Society of Cardiology

Cardiovascular Research (2019) **115**, 419–431
doi:10.1093/cvr/cvy200

Peroxisome proliferator-activated receptor-gamma targeting nanomedicine promotes cardiac healing after acute myocardial infarction by skewing monocyte/macrophage polarization in preclinical animal models

Masaki Tokutome[1], Tetsuya Matoba[1]*, Yasuhiro Nakano[1], Arihide Okahara[1], Masaki Fujiwara[1], Jun-Ichiro Koga[2], Kaku Nakano[2], Hiroyuki Tsutsui[1], and Kensuke Egashira[1,2]

[1]Department of Cardiovascular Medicine, Kyushu University Graduate School of Medical Sciences, 3-1-1, Maidashi, Higashi-ku, Fukuoka 812-8582, Japan; and [2]Department of Cardiovascular Research, Development, and Translational Medicine, Center for Disruptive Cardiovascular Medicine, Kyushu University, Fukuoka, Japan

Received 29 July 2017; revised 6 June 2018; editorial decision 26 July 2018; accepted 1 August 2018; online publish-ahead-of-print 3 August 2018

Time for primary review: 46 days

Aims Monocyte-mediated inflammation is a major mechanism underlying myocardial ischaemia–reperfusion (IR) injury and the healing process after acute myocardial infarction (AMI). However, no definitive anti-inflammatory therapies have been developed for clinical use. Pioglitazone, a peroxisome proliferator-activated receptor-gamma (PPARγ) agonist, has unique anti-inflammatory effects on monocytes/macrophages. Here, we tested the hypothesis that nanoparticle (NP)-mediated targeting of pioglitazone to monocytes/macrophages ameliorates IR injury and cardiac remodelling in preclinical animal models.

Methods and results We formulated poly (lactic acid/glycolic acid) NPs containing pioglitazone (pioglitazone-NPs). In a mouse IR model, these NPs were delivered predominantly to circulating monocytes and macrophages in the IR heart. Intravenous treatment with pioglitazone-NPs at the time of reperfusion attenuated IR injury. This effect was abrogated by pre-treatment with the PPARγ antagonist GW9662. In contrast, treatment with a pioglitazone solution had no therapeutic effects on IR injury. Pioglitazone-NPs inhibited Ly6C^{high} inflammatory monocyte recruitment as well as inflammatory gene expression in the IR hearts. In a mouse myocardial infarction model, intravenous treatment with pioglitazone-NPs for three consecutive days, starting 6 h after left anterior descending artery ligation, attenuated cardiac remodelling by reducing macrophage recruitment and polarizing macrophages towards the pro-healing M2 phenotype. Furthermore, pioglitazone-NPs significantly decreased mortality after MI. Finally, in a conscious porcine model of myocardial IR, pioglitazone-NPs induced cardioprotection from reperfused infarction, thus providing preclinical proof of concept.

Conclusion NP-mediated targeting of pioglitazone to inflammatory monocytes protected the heart from IR injury and cardiac remodelling by antagonizing monocyte/macrophage-mediated acute inflammation and promoting cardiac healing after AMI.

Keywords Myocardial infarction • Ischaemia reperfusion • Inflammation • Macrophage

* Corresponding author. Tel: +81 92 642 5360; fax: +81 92 642 5374, E-mail: matoba@cardiol.med.kyushu-u.ac.jp

1. Introduction

Acute myocardial infarction (AMI) is a major cause of death and heart failure worldwide.[1] Early reperfusion therapy is the standard strategy for restoring the myocardium after ischaemia in AMI. Although the door-to-balloon time for reperfusion therapy has been shortened in recent years, the mortality rate has not improved.[2] The reperfusion of occluded coronary arteries induces myocardial ischaemia–reperfusion (IR) injury, which enlarges infarct sizes and negates the beneficial effects of reperfusion.[3,4] Larger infarct sizes lead to left ventricular (LV) remodelling and heart failure. Several mechanisms underlying myocardial IR injury have been identified, including calcium overload, rapid pH correction, and reactive oxygen species (ROS) generation, all of which cause mitochondrial injury and thus lead to cardiomyocyte necrosis and apoptosis. ROS and cellular injury cause acute inflammation that leads to cardiomyocyte apoptosis.[3–5] After cardiomyocyte death, the heart begins to repair itself. Inflammatory cells infiltrate the heart and remove dead cardiomyocytes. After the resolution of the inflammatory response, cardiac fibroblasts proliferate and secrete extracellular matrix proteins, which form a fibrotic scar that replaces the dead cardiomyocytes. The resulting tightly cross-linked fibrotic scar prevents rupture. This progressive LV remodelling continues in response to increases in wall stress and thus provokes cardiomyocyte hypertrophy in the infarct border zone, wall thinning, and chamber dilation. This adverse remodelling response leads to increased LV volumes and reduced ejection fractions.[6] As of the writing of this manuscript, cardioprotective agents that have been efficacious in animal models have not been so in clinical trials.[7,8] These circumstances prompted us to develop novel therapeutic modalities to protect the heart from IR injury and cardiac remodelling. To this end, we accomplished the following two objectives in this study: (i) we defined new therapeutic targets and (ii) we applied a drug delivery system (DDS).

Cardiac inflammation plays important roles in both IR injury and cardiac remodelling after MI. Recent reports, including ours,[9–11] have indicated that inflammatory monocytes play roles in acute cardiac inflammation, which enlarges infarct sizes during IR injury; therefore, suppressing acute monocyte-mediated inflammation reduces IR injury. Macrophages can be divided into at least the following two subsets: classically activated/pro-inflammatory M1 macrophages, whose differentiation is stimulated by IFNγ or lipopolysaccharide, and alternatively activated/pro-healing M2 macrophages, whose differentiation is stimulated by IL-4 or IL-13. Depleting the total macrophages from the infarcted hearts by using clodronate liposomes impairs collagen deposition, necrotic cell clearance, and angiogenesis, thus predisposing affected individuals to cardiac rupture and death.[12] These findings indicate that pro-healing M2 macrophages are essential for the cardiac healing process. Therefore, inhibiting pro-inflammatory macrophage functions and inducing pro-healing macrophage functions are critical in the development of new therapies for myocardial IR injury.

To fulfil our objectives, we focused on peroxisome proliferator-activated receptor-gamma (PPARγ), a member of the nuclear receptor family. Ligands, including pioglitazone, bind to PPARγ and form heterodimers with another nuclear receptor, retinoid X receptor (RXR). This heterodimer binds to the PPAR response element and regulates downstream genes that participate in adipogenesis and lipid/glucose metabolism.[13–15] Additionally, the PPARγ/RXR heterodimer causes NF-κB and AP-1 transrepression, thus resulting in reductions in chemokine expression and macrophage infiltration into injured organs.[16,17] In monocytes/macrophages, PPARγ activation skews macrophages towards the pro-healing M2 macrophage phenotype via NF-κB inhibition.[18–20] These findings suggest the potential anti-inflammatory and pro-healing effects of PPARγ agonists in myocardial IR injury.

Pioglitazone, a clinically approved thiazolidinedione, is a potent PPARγ agonist. In a previous report, oral pioglitazone started 3 or 14 days before ischaemia induction reduced infarct sizes in mouse and rat myocardial IR injury models[21,22]; however, pioglitazone did not have therapeutic effects when it was administered intraperitoneally at the time of reperfusion.[22] Because cardioprotective agents are administered during reperfusion therapy, it is essential to use a DDS that facilitates pioglitazone delivery to the cells that are responsible for IR injury. We have developed a nanoparticle (NP)-mediated DDS consisting of a bioabsorbable poly (lactic-co-glycolic acid) (PLGA) polymer.[23–28] PLGA-NPs extravasate and accumulate in the ischaemia-reperfusion myocardium via enhanced vascular permeability and are taken up by circulating monocytes via phagocytosis. Phagocytosis is a primary mechanism for NP uptake by monocytes/macrophages.[29] We have also reported previously that compared with bare pioglitazone, pioglitazone-NPs better inhibit matrix metalloproteinase (MMP) activity by regulating monocyte/macrophage activation in hyperlipidaemic ApoE$^{-/-}$ mice, thus suggesting that PLGA-NPs are a feasible DDS for targeting inflammatory monocytes/macrophages.[30] These properties of PLGA NPs may enhance the therapeutic effects of pioglitazone, namely, its anti-inflammatory effects that reduce infarct sizes during the acute phase and its pro-healing effects that reduce adverse LV remodelling during the chronic phase.

In the present study, we first showed that pioglitazone-NPs exert anti-inflammatory effects that limit the infarct size in an IR model in mice. Then, we demonstrated the effects of pioglitazone-NPs on cardiac remodelling in an MI model in mice. Finally, we tested the therapeutic effects of pioglitazone-NPs in a preclinical porcine IR model.

2. Methods

2.1 Preparation of PLGA NPs

PLGA NPs encapsulated with fluorescein isothiocyanate (FITC; Dojin Chemical, Tokyo, Japan) (FITC-NPs) and pioglitazone (Takeda Pharmaceutical Company Limited, Osaka, Japan) (pioglitazone-NPs) were prepared using emulsion solvent diffusion as previously reported.[27,31] FITC-NPs were 4.05% (wt/vol) FITC, and pioglitazone-NPs were 4.95% (wt/vol) pioglitazone. Additional details can be found in the Supplementary material online.

2.2 Mouse and porcine myocardial IR injury model and MI model

Adult male C57BL/6J mice (9–13 weeks old) (CLEA Japan, Inc.), C-C chemokine receptor 2 (CCR2)-deficient mice on a C57BL/6J background, and Chinese Bama mini-pigs (age: 4–6 months, BW: 10–15 kg) were used in this study. The mouse experiments were reviewed and approved by the Ethics Committee on Animal Experiments, Kyushu University Faculty of Medicine, and were conducted according to the American Physiological Society guidelines and the NIH guide for the care and use of laboratory animals, 8th edition. The Bama mini-pig experiment was conducted by JOINN Laboratories Inc. (http://www.joinnlaboratories.com/home/index2.html) in Suzhou, China. JOINN was accredited by the AAALAC in 2011 by the Chinese FDA. This experiment was reviewed and approved by the local ethics committee of JOINN Laboratories. The myocardial IR model was established on the basis of previously described methods.[32–34] Additional details for each experimental protocol can be found in the Supplementary material online.

2.3 Measurements of pioglitazone concentrations in plasma and tissues

After animals were euthanized with intraperitoneal pentobarbital administration at 200 mg/kg at predetermined time points, pioglitazone concentrations in the plasma and tissues were measured with liquid chromatography coupled to tandem mass spectrometry (LC/MS/MS). Additional details can be found in the Supplementary material online.

2.4 Histological and immunohistochemical analysis

Twenty-four hours after reperfusion, the hearts were harvested and fixed overnight in 10% buffered formalin. After fixation, the tissues were embedded in paraffin. Serial cross-sections (5 μm thick) were used for analysis. The sections were subjected to immunohistology using an anti-MCP-1 antibody (1:200, Santa Cruz Biotechnology) and anti-CD11b antibody (1:200, BD Biosciences).

2.5 PPARγ and NF-κB activity in the myocardium

Nuclear extracts were prepared from myocardial homogenates with a nuclear extract kit (NE-PER Nuclear and Cytoplasmic Extraction Reagents; Thermo Fisher Scientific Inc., Rockford, IL, USA) according to the manufacturer's instructions. PPARγ and NF-κB activation were assayed using an ELISA-based PPARγ Activation TransAM Kit (Active Motif, Rixensart, Belgium) and an ELISA-based NF-κB Activation TransAM Kit (Active Motif, Rixensart, Belgium), according to the manufacturer's instructions. Additional details can be found in the Supplementary material online.

2.6 Real-time PCR

Real-time PCR (RT-PCR) was performed with SYBR Premix DimerEraser (Perfect Real-time, TAKARA BIO Inc.) and a StepOnePlus Real-time PCR System (Applied Biosystems, MA, USA). Additional details can be found in the Supplementary material online.

2.7 FMT and fluorescence reflectance imaging

We used the activated fluorescence imaging agents Prosense-680 (Ex/Em = 680/700 nm) and MMPSense-750 (Ex/Em = 749/775 nm) (PerkinElmer, Inc., Waltham, MA, USA) for this portion of the study. The animals were anesthetized via isoflurane (1.5%) inhalation and were scanned with an FMT-2000 system (PerkinElmer, Inc., Waltham, MA, USA). Additional details can be found in the Supplementary material online.

2.8 Flow cytometry

Leucocytes from the peripheral blood, spleen, and heart were obtained from mice and analysed with a Gallios Flow Cytometer (Beckman Coulter, Inc., CA, USA). Additional details can be found in the Supplementary material online.

2.9 Echocardiography

At predetermined time points, we used a 12-MHz probe (Visualsonics, Ontario, Canada) to perform transthoracic two-dimensional echocardiography on mice anesthetized via isoflurane (1%) inhalation; the mice were maintained at a heart rate of approximately 500 b.p.m. Additional details can be found in the Supplementary material online.

2.10 Statistical analysis

The data are expressed as the mean ± SE. Statistical analyses of the differences between two groups were performed using the unpaired *t*-test, and analyses of the differences among three groups were performed by ANOVA, followed by the Bonferroni's *post hoc* multiple comparison test, using Prism Software version 4.0 (Graph Pad Software, San Diego, California, USA). Any *P* values less than 0.05 were considered to be significant.

3. Results

3.1 PLGA-NP delivery in a myocardial IR model

At 30 min after coronary ligation in mice, we intravenously administered the FITC solution or FITC-NPs at the time of reperfusion (Experimental Protocol 1, Supplementary material online, *Figure S2*). We examined FITC signals in leucocytes in the blood, spleen, and heart at 6 h after reperfusion by using flow cytometry to determine the uptake of FITC-NPs by the monocytes in these samples (*Figure 1A*). We next examined the histological distribution of FITC-NPs in the IR heart. Strong FITC signals were detected in the area at risk (AAR) of the IR hearts in the FITC-NP group, whereas no FITC signals were detected in the hearts of the saline and FITC solution groups (*Figure 1B*). Immunofluorescence analysis confirmed the presence of FITC signals in troponin T-positive cardiomyocytes (*Figure 1B*). FITC signals were significantly less intense in the non-ischaemic area than in the ischaemic area. Moreover, transmission electron microscopy analysis in mouse hearts 30 min after IR revealed that NPs were localized to lysosomes in the IR-injured myocardium (Supplementary material online, *Figure S3*). Next, we examined the plasma and tissue concentrations of pioglitazone in mice after the intravenous administration of pioglitazone solution (1.0 mg/kg) or pioglitazone-NPs (containing 1.0 mg/kg pioglitazone). The tissue concentrations of pioglitazone measured 30 min after reperfusion in the IR myocardium and spleen were higher in the pioglitazone-NP group than in the pioglitazone group (*Figure 1C*). Pioglitazone concentrations in the IR myocardium were higher than those in the non-ischaemic myocardium in the pioglitazone-NP group at 30 min after reperfusion (*Figure 1C*). Furthermore, pioglitazone concentrations in the liver and kidneys were equivalent in the pioglitazone and pioglitazone-NP groups (Supplementary material online, *Figure S4*). These data indicate that (i) PLGA-NPs deliver pioglitazone to monocytes in the blood, spleen, and IR heart, (ii) PLGA-NPs deliver pioglitazone to the IR myocardium, and (iii) tissue pioglitazone concentrations were higher in the IR myocardium and spleen after the intravenous administration of pioglitazone-NPs.

3.2 Pioglitazone-NPs reduced myocardial IR injury via a PPARγ-dependent mechanism

We evaluated the therapeutic effects of pioglitazone and pioglitazone-NPs administered at the time of reperfusion on reducing myocardial IR injury in mice (Experimental Protocol 2, Supplementary material online, *Figure S2*). Consistent with the results from a previous report, intravenously administered pioglitazone solution at doses up to 3.0 mg/kg showed no therapeutic effects (*Figure 2A*, left).[22] Importantly, single intravenous treatments with pioglitazone-NPs (containing 0.1–3.0 mg/kg pioglitazone) reduced the infarct sizes evaluated 24 h after reperfusion

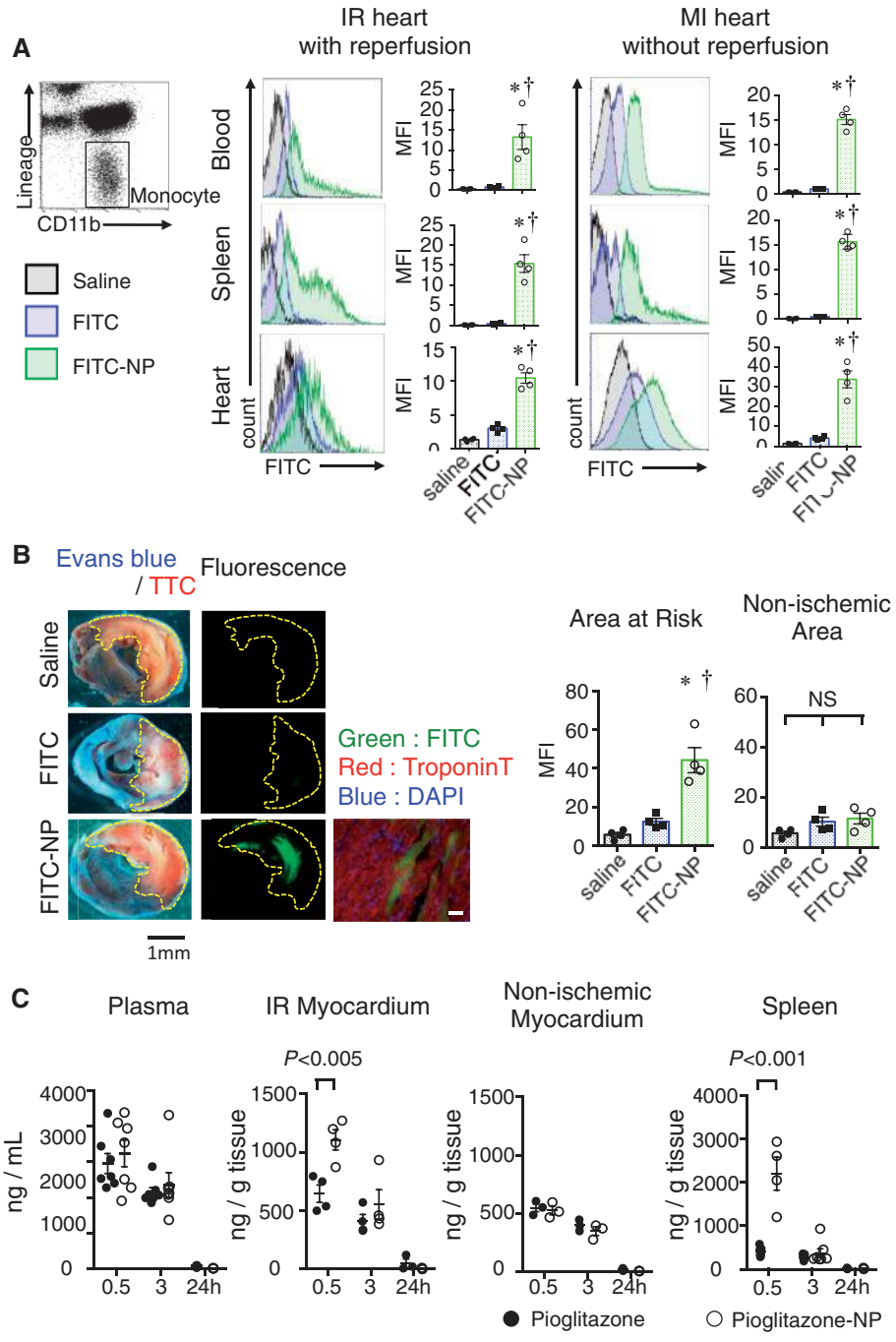

Figure 1 PLGA nanoparticles as a drug delivery system for IR injury. (*A*) Histograms illustrating the uptake of FITC-NPs (green) in the respective cells (columns) and organs (rows). Column graphs illustrating the quantification of FITC mean fluorescence intensity (MFI) in the respective cells. The data are shown as the mean ± SE ($N = 4$ mice per group). *$P < 0.0001$ vs. saline, †$P < 0.05$ vs. FITC using one-way ANOVA followed by Bonferroni's multiple comparison test. (*B*) Representative light (left) and fluorescence (right) stereomicrographs of whole hearts 3 h after the intravenous injection of FITC-NPs. White indicates the MI area (TTC-negative), red indicates the non-MI area within the AAR, and blue indicates the non-ischaemic area. Fluorescence photomicrographs of cross-sections from hearts treated with FITC-NPs. Green indicates FITC, red indicates troponin T, and blue indicates DAPI. Scale bar: 20 µm. Column graphs illustrating the quantification of FITC MFI in the AAR and non-ischaemic area. The data are shown as the mean ± SE ($N = 4$ mice per group). *$P < 0.001$ vs. saline, †$P < 0.001$ vs. FITC using one-way ANOVA, followed by Bonferroni's multiple comparison test. (*C*) Plasma, myocardial tissue (AAR, non-ischaemic area), and spleen concentrations of pioglitazone after 30 min, 3 h, and 24 h of intravenous injections of pioglitazone alone or pioglitazone-NPs. The data are shown as the mean ± SE ($N = 4$ mice per group). The data were compared using two-way ANOVA, followed by Bonferroni's multiple comparison test.

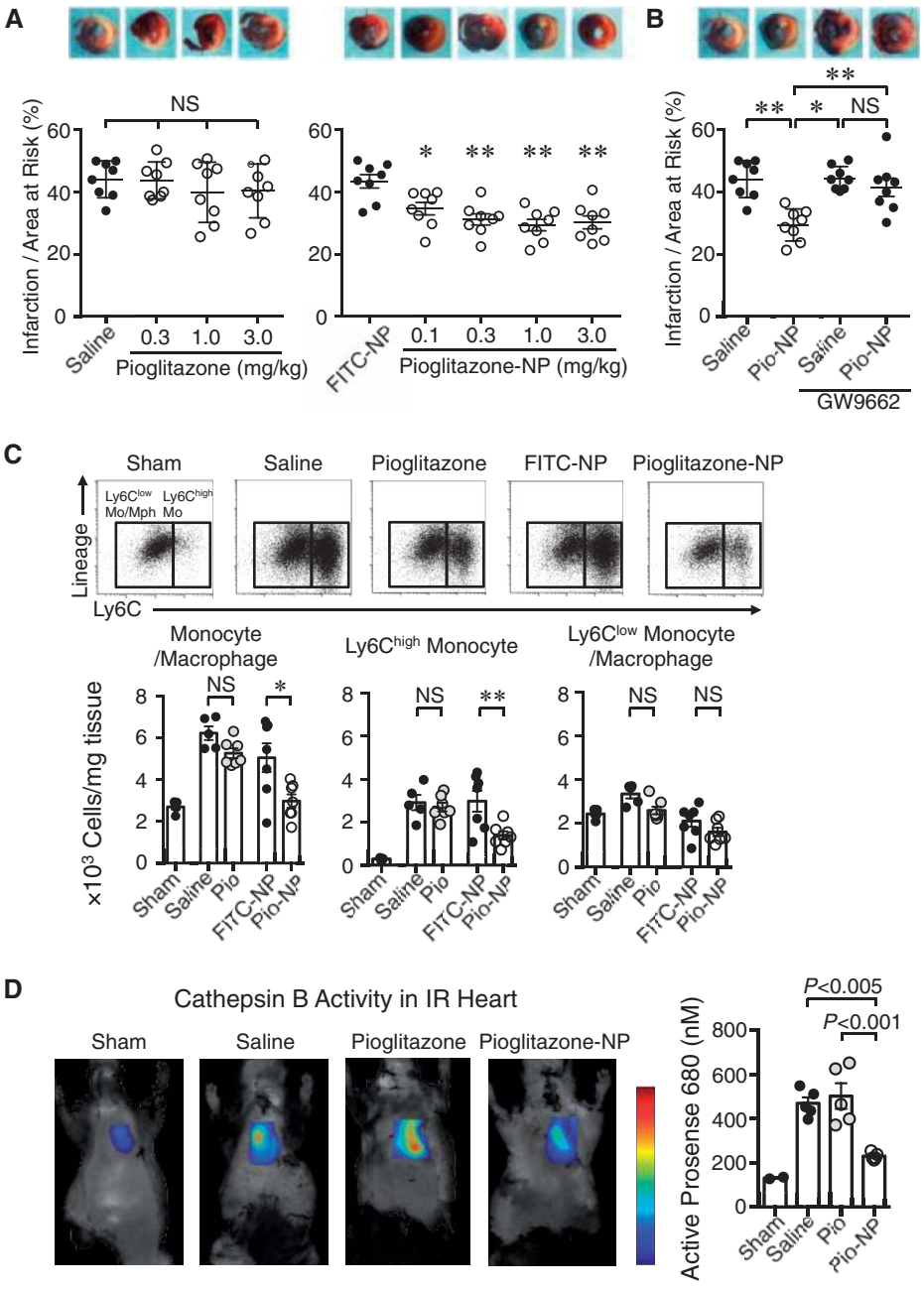

Figure 2 Therapeutic effects of pioglitazone-NPs on IR injury. (*A*) The effects of saline, FITC-NPs, pioglitazone alone, and pioglitazone-NPs on infarct size after IR. The data are expressed as the mean ± SE ($N = 8$ per group). $^{*}P < 0.05$ and $^{**}P < 0.001$ vs. the FITC-NP group using one-way ANOVA, followed by Bonferroni's multiple comparison test. NS, not significant. (B) The effects of the PPARγ antagonist GW9662 on the therapeutic effects of pioglitazone-NPs on MI size. The data are expressed as the mean ± SD ($N = 8$ per group). $^{*}P < 0.005$ and $^{**}P < 0.001$ using one-way ANOVA, followed by Bonferroni's multiple comparison test. NS, not significant. (*C*) Flow cytometric analysis of the leucocytes in IR hearts treated with saline, FITC-NPs, pioglitazone alone, and pioglitazone-NPs. $^{*}P < 0.05$ and $^{**}P < 0.01$ using one-way ANOVA followed by Bonferroni's multiple comparison tests. (*D*) Coronal FMT image acquired 24 h after the injection of Prosense-680 demonstrating strong fluorescence in the cardiac region in IR mice. Quantification of Prosense-680 activation 48 h after IR. The data are reported as the mean ± SE ($N = 5$ per group). The data were compared using one-way ANOVA, followed by Bonferroni's multiple comparison test. FMT, fluorescence molecular tomography.

(*Figure 2A*, right). The infarct-limiting effect of pioglitazone-NPs was abrogated by pre-treatment with the PPARγ antagonist GW9662 (2.0 mg/kg) (*Figure 2B*); these data indicated that pioglitazone-NPs reduced myocardial IR injury mainly via PPARγ-dependent mechanisms. Treatment with pioglitazone-NPs or pioglitazone alone did not affect the AAR in the hearts (Supplementary material online, *Figure S5*). Moreover, treatment with pioglitazone-NPs had no effects on lipid levels (Supplementary material online, *Figure S6*).

3.3 Pioglitazone-NPs antagonized monocyte/macrophage-mediated inflammation in a mouse IR model

Thiazolidinediones are known to repress NF-κB, which regulates inflammation, including monocyte/macrophage chemotaxis.[17,35] Therefore, we examined the effects of pioglitazone-NPs on leucocyte recruitment by flow cytometry with a gating strategy to differentiate monocyte/macrophages from other cells in the heart (Experimental Protocol 2, Supplementary material online, *Figures S2* and *S7*). Flow cytometric analysis performed 24 h after reperfusion revealed that pioglitazone-NPs significantly reduced the numbers of total monocytes/macrophages and Ly6C^{high} inflammatory monocytes in the heart (*Figure 2C*). Macrophages produce several proteinases, including cathepsins, which degrade the extracellular matrix and promote LV dilation. We performed molecular imaging with FMT using Prosense, an indicator of cathepsin B activity, in the IR heart (Experimental Protocol 3, Supplementary material online, *Figure S2*). Pioglitazone-NPs containing 1 mg/kg pioglitazone reduced cathepsin B activity in the IR hearts, whereas the same dose of pioglitazone solution did not affect cathepsin B activity (*Figure 2D*).

Pioglitazone-NPs increased PPARγ DNA-binding activity in the myocardium nuclear extracts after ischaemia, but pioglitazone solution did not increase PPARγ DNA-binding activity (*Figure 3A*). Furthermore, pioglitazone-NPs decreased NF-κB DNA-binding activity in the myocardium after ischaemia (*Figure 3B*). Pioglitazone-NPs significantly decreased MCP-1, TNFα, iNOS, COX2, Nlrp3, and ICAM1 gene expression levels in the IR heart (*Table 1*). Histological analysis revealed that most of the MCP-1-positive area was not co-stained with CD11b, indicating that MCP-1 was expressed by mainly the cardiomyocytes in the IR hearts (*Figure 3D*). Pioglitazone-NPs reduced the recruitment of leucocytes expressing MCP-1 after IR injury (*Figure 3E*) and decreased the number of MCP-1-expressing cardiomyocytes (*Figure 3F*).

3.4 CCR2-dependent inflammatory monocyte recruitment is the primary target of pioglitazone-NPs

MCP-1 is a potent monocyte chemokine, and deletion of its receptor CCR2 inhibits monocyte-mediated inflammation in various situations, including IR injury.[11,36] Therefore, we have evaluated the therapeutic efficacy of pioglitazone-NPs in CCR2$^{-/-}$ mice to explore the primary therapeutic target of pioglitazone-NPs, i.e. monocytes vs. non-monocytes, including cardiomyocytes (Experimental Protocol 2, Supplementary material online, *Figure S2*). Flow cytometry showed the recruitment of Ly6C^{high} monocytes to the IR hearts at 24 h after reperfusion in WT mice, and this effect was blunted in CCR2$^{-/-}$ mice (*Figure 3G*). Pioglitazone-NPs did not decrease the number of Ly6C^{high} monocytes or the gene expression levels of inflammatory genes in the hearts of CCR2$^{-/-}$ mice (*Figure 3G* and *Table 1*). Importantly, pioglitazone-NPs did not further reduce IR injury in CCR2$^{-/-}$ mice compared with that in the saline group (*Figure 3H*). These results indicate that the MCP-1/CCR2-dependent recruitment of inflammatory monocytes is the primary therapeutic target of pioglitazone-NPs.

3.5 Pioglitazone-NP effects on both cardiomyocytes and monocytes

We examined whether pioglitazone-NPs have direct effects on MCP-1 expression in cardiomyocytes. In *ex vivo* cultured primary mouse cardiomyocytes, pioglitazone-NPs decreased MCP-1 concentrations after hypoxia-reoxygenation in culture supernatants (Supplementary material online, *Figure S8*).

Then, we examined the effects of pioglitazone-NPs on inflammation in monocytes from the peripheral blood. Flow cytometric analysis performed 3 days after ligation of the left anterior descending (LAD) artery revealed that pioglitazone-NPs decreased the number of Ly6C^{high} monocytes, which represent the 'inflammatory' monocyte subset, whereas Ly6C^{low} 'non-inflammatory' monocytes showed no significant difference between the two groups. The total monocyte count was not affected. As a result, the peripheral monocyte polarity defined as Ly6C^{high} monocytes/Ly6C^{low} monocytes was significantly altered towards a less inflammatory state (Supplementary material online, *Figure S9*). Furthermore, pioglitazone-NPs inhibited THP-1 monocyte chemotaxis to MCP-1 (Supplementary material online, *Figure S10*), indicating that pioglitazone-NPs exerted effects on monocytes/macrophages. Therefore, pioglitazone-NPs affect both cardiomyocytes and monocytes/macrophages.

3.6 Pioglitazone-NP effects on myocardial function and remodelling in a mouse IR model

Echocardiography performed 4 weeks after IR showed that both LV end-diastolic dimension (LVEDD) and LV end-systolic dimension (LVESD) were significantly increased in the vehicle group. In contrast, intravenous treatment with pioglitazone-NPs, but not pioglitazone alone, at the time of reperfusion reduced the above increases in LVEDD and LVESD at 2 and 4 weeks after IR in the treatment groups (*Figure 4A* and *B*, Supplementary material online, *Table S1*). Pioglitazone-NPs, but not pioglitazone alone, attenuated the above decreases in the LV ejection fraction (LVEF) and LV fractional shortening (LVFS) at 2 and 4 weeks after IR (Figure 4A and *B*, Supplementary material online, *Table S1*).

3.7 Pioglitazone-NP effects on myocardial remodelling and survival in a mouse MI model

We examined the effects of pioglitazone-NPs on cardiac remodelling and survival in a mouse MI model. In this mouse MI model, drugs were administered by intravenous injection for three consecutive days, starting 6 h after LAD ligation, when myocardial infarction was complete (Experimental Protocol 5, Supplementary material online, *Figure S2*). There were significant differences in the infarct sizes between the two groups on Day 1 after MI (*Figure 5A*). Histological analysis showed that pioglitazone-NPs reduced Masson-trichrome-positive scar areas and fibrosis in the border zone (*Figure 5B*). Pioglitazone-NPs reduced the aforementioned increases in LVEDD and LVESD and attenuated the aforementioned decreases in LVEF and LVFS at 28 days after MI (Figure 5C and *D*, Supplementary material online, *Table S2*). The mortality rate was significantly higher in the saline group (58%) than in the pioglitazone-NP group (37%) at 28 days after LAD ligation. Statistical analyses indicated that pioglitazone-NPs significantly decreased mortality after MI (*Figure 5E*). We also found that pioglitazone-NPs significantly decreased mortality due to ventricular rupture (*Figure 5F*).

3.8 Pioglitazone-NPs induced macrophage polarization toward a pro-healing M2 phenotype in a mouse MI model

We examined FITC signals in leucocytes after treatment with FITC solution or FITC-NPs for three consecutive days, starting 6 h after

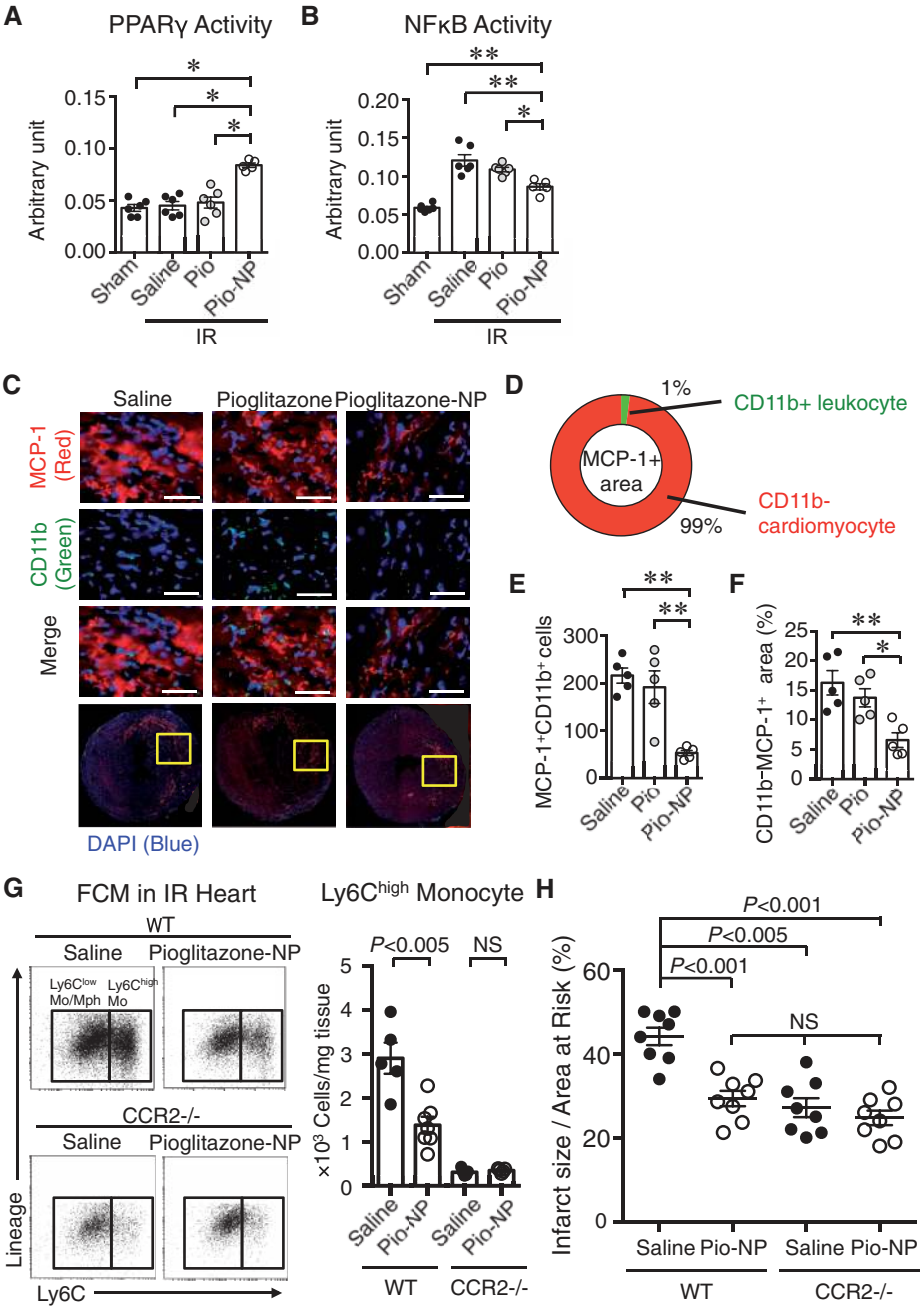

Figure 3 Anti-inflammatory effects of pioglitazone-NPs on IR injury. (*A*) PPARγ activity in the myocardium after ischaemia at 6 h after reperfusion. The data are expressed as the mean ± SE ($N = 6$ per group). *$P < 0.001$ using one-way ANOVA followed by Bonferroni's multiple comparison test. (*B*) NF-κB activation in the myocardium after ischaemia at 6 h after reperfusion. The data are expressed as the mean ± SE ($N = 6$ per group). *$P < 0.05$ and **$P < 0.005$ using one-way ANOVA followed by Bonferroni's multiple comparison test. (*C*) Representative fluorescent immunostaining images. Hearts at 12 h after IR injury were stained with anti-MCP-1 antibody (red), anti-CD11b antibody (green), and DAPI (blue). The rectangles in the lower panels indicate the magnified area in the above pictures. (*D*) Quantitative assessment of the cell types in MCP-1-positive cells. (*E*) Quantitative assessment of MCP-1-positive and CD11b-positive leucocytes. The data indicate the cell number per high power field. (*F*) Quantitative assessment of MCP-1-positive cardiomyocytes (CD11b-negative cells). The data indicate the percentage MCP-1-positive area in cardiomyocytes. The data are expressed as the mean ± SE ($N = 6$ per group). *$P < 0.05$ and **$P < 0.01$ using one-way ANOVA followed by Bonferroni's multiple comparison test. Scale bar: 20 μm. (*G*) The effects of pioglitazone-NPs on monocyte recruitment in WT and CCR2$^{-/-}$ mice. The data are expressed as the mean ± SE ($N = 5$ per group). The data were compared using two-way ANOVA followed by Bonferroni's multiple comparison test. NS, not significant. (*H*) The effects of pioglitazone-NPs on IR injury in CCR2$^{-/-}$ mice. The data are expressed as the mean ± SE ($N = 8$ per group). The data were compared using two-way ANOVA followed by Bonferroni's multiple comparison test. NS, not significant.

Table 1 Pioglitazone-NP effects on the mRNA levels of inflammatory and adhesion molecules in IR hearts in WT and CCR2$^{-/-}$ mice after IR

	Fold change					
	WT			CCR2$^{-/-}$		
Gene	Saline	Pio-NP	*P*-value	Saline	Pio-NP	*P*-value
Inflammation						
MCP-1	34.1***	12.3*	<0.001	6.4	5.6	NS
TNFα	5.4***	2.4**	<0.001	1.5	1.7	NS
IL1β	27.2***	23.1	NS	5.3****	7.5	NS
IL6	64.1**	36.2	NS	19.0	19.9	NS
iNOS	9.0***	3.9*	<0.001	3.2	3.9	NS
COX2	6.2***	3.3**	<0.005	1.9	2.6	NS
Nlrp3	6.9***	3.7	<0.05	1.6	1.9	NS
Adhesion molecules						
ICAM1	4.0***	2.1	<0.01	1.8	2.1	NS
VCAM1	2.8***	2.1**	NS	1.6	1.9	NS
P-selectin	18.7*	14.6	NS	8.0	9.4	NS
E-selectin	5.2***	3.1	NS	1.5	1.8	NS

The data were normalized to the sham-operated controls ($N = 6$: WT, $N = 5$: CCR2$^{-/-}$).
*$P < 0.05$ vs. the sham group using one-way ANOVA followed by Bonferroni's multiple comparison test.
**$P < 0.01$ vs. the sham group using one-way ANOVA followed by Bonferroni's multiple comparison test.
***$P < 0.001$ vs. the sham group using one-way ANOVA followed by Bonferroni's multiple comparison test.
****$P < 0.05$ vs. the WT pioglitazone-NP group using one-way ANOVA followed by Bonferroni's multiple comparison test.

LAD ligation. Flow cytometric analysis of leucocytes in the blood, spleen, and heart revealed the uptake of FITC-NPs by monocytes in the blood, spleen, and heart, thus indicating that PLGA NPs were delivered to inflammatory monocytes in the mouse MI model (*Figure 1A*).

Next, we examined the effect of pioglitazone-NPs on monocytes/macrophages in the mouse MI model. Flow cytometric analysis performed 3 days after LAD ligation revealed that pioglitazone-NPs significantly reduced the numbers of Ly6C^{high} inflammatory monocytes, Ly6C^{low} monocytes and M1 macrophages in the heart (*Figure 6A*). Pioglitazone-NPs decreased the percentage of M1 macrophages in the acute inflammatory phase on Day 3 and increased the percentage of M2 macrophages in the repair phase on Day 7 (*Figure 6B*). MMP is a potential biomarker for LV expansion. Therefore, we examined MMP expression and activity. Pioglitazone-NPs increased TIMP1 expression and decreased MMP2 expression, as determined by RT-PCR (*Figure 6C*). FMT revealed that pioglitazone-NPs decreased cathepsin B activity (*Figure 6D*) and MMP activity in mouse MI hearts (*Figure 6E*). Collectively, these data suggest that pioglitazone-NPs reduced macrophage recruitment, polarized macrophages towards a pro-healing state, and decreased MMP activity in the heart after MI; these effects thus attenuated cardiac dilatation and dysfunction.

3.9 Pioglitazone-NPs reduced reperfused infarction in a porcine model

To translate the above findings into a clinical setting, we examined the effects of pioglitazone-NPs in a conscious porcine model. A cuff occluder was implanted into the left circumflex coronary, and occlusion was performed for 1 hour (*Figure 7A*). Intravenous treatment with pioglitazone-NPs at 0.3 mg/kg at the time of reperfusion reduced the MI size (*Figure 7B*). The AAR percentages in the ventricles were comparable among the study groups. Treatment with pioglitazone-NPs exerted no effects on the arterial blood pressure and heart rate (Supplementary material online, *Table S3*). Moreover, we observed no significant differences in the incidence of ventricular arrhythmias (premature ventricular contraction and non-fatal ventricular tachycardia) among the treatment groups (Supplementary material online, *Table S4*).

4. Discussion

The novel findings of the present study are as follows: pioglitazone-NPs (i) attenuated CCR2^{+} monocyte-mediated acute inflammation and reduced infarct sizes in a mouse IR injury model, (ii) promoted macrophage polarization towards a pro-healing M2 phenotype and attenuated cardiac remodelling in an MI model without reperfusion, and (iii) induced cardioprotection in a conscious mini-pig model of myocardial IR injury. These findings provide a pre-clinical proof of concept.

PLGA-NPs play a critical role as a DDS in myocardial IR injury. FITC-NPs were delivered to circulating monocytes and macrophages in the IR hearts (*Figure 1A* and *B*). In accordance with our results regarding FITC-NP distributions, our results regarding pioglitazone concentrations suggest that PLGA-NPs can modulate the *in vivo* kinetics of pioglitazone (*Figure 1C*). The findings of our previous studies have suggested that PLGA-NP delivery is dependent on enhanced vascular permeability and phagocytosis by mononuclear phagocytic systems, including circulating monocytes and splenic monocytes/macrophages that are potential sources of Ly6C^{high} monocytes that are recruited to the IR myocardium.[11,28] In the MI hearts without reperfusion, drugs cannot reach the myocardium after ischaemia. We found that PLGA-NPs delivered FITC or pioglitazone to monocytes/macrophages in the blood, spleen, and MI heart without reperfusion (*Figure 1A*), indicating that PLGA NP-mediated DDS delivered incorporated agents to monocytes before their recruitment to the MI hearts. Furthermore, the spleen is a monocyte reservoir, and recent studies have demonstrated monocyte mobilization from the spleen to the ischaemic heart in the acute phase after MI,[37,38] thus indicating that PLGA-NPs delivered to splenic monocytes may inhibit monocyte activation and the resultant monocyte recruitment to the heart after MI.

We demonstrated that pioglitazone-NPs reduced IR injury by inhibiting inflammatory monocyte recruitment from the peripheral blood to the heart tissue and reducing inflammatory gene expression (*Figure 2A* and *B*, and *Table 1*). In contrast, pioglitazone alone at the same dose failed to increase PPARγ activity (*Figure 3A*) and inhibit IR injury (*Figure 2A*). The primary mechanism by which pioglitazone-NP showed superior efficacy appears to be enhanced drug delivery to cardiomyocytes, peripheral monocytes, and macrophages in the heart to activate PPARγ.

In the present study, PPARγ activity was not increased after IR (*Figure 3A*). We have previously reported that the PPARγ antagonist GW9662 did not decrease PPARγ activity in the heart after IR,[11] suggesting that PPARγ activity is not involved in NF-κB activation after myocardial IR injury in this model. NF-κB activation during IR is attributable to the DAMP-mediated activation of the TLR4-NF-κB pathway.[39] In addition, it has been reported that the induction of endogenous PPARγ is insufficient to increase PPAR target genes associated with cardiac energy metabolism after permanent coronary artery ligation in Sprague Dawley rats.[40] These observations suggest the minor role of

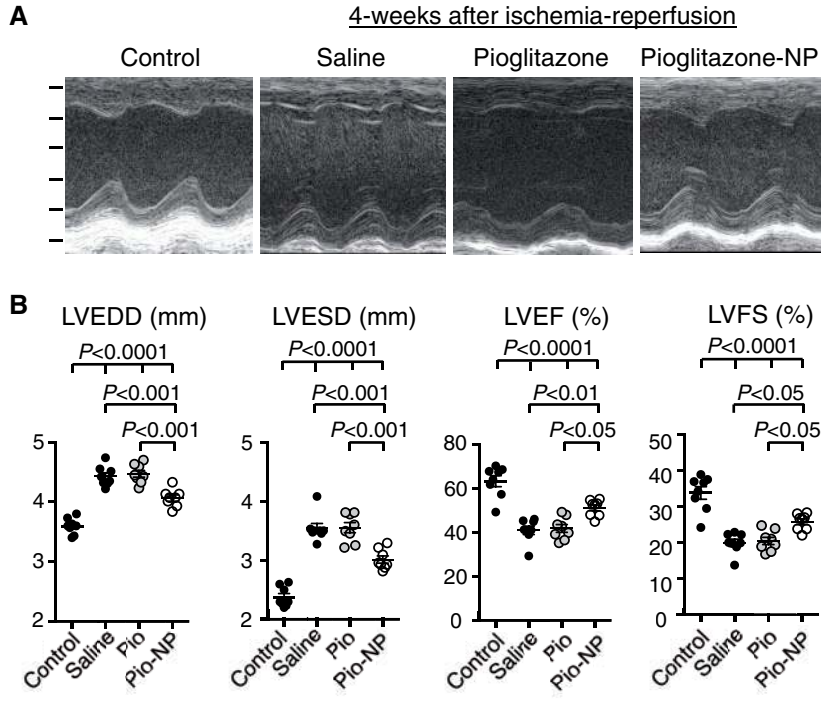

Figure 4 Pioglitazone-NP effects on myocardial remodelling in a mouse IR model. (*A*) Representative M-mode echocardiograms for animals treated with pioglitazone alone or pioglitazone-NPs at 4 weeks after reperfusion. The interval of the scale is 1 mm. (*B*) Pioglitazone-NP effects on LVEDD, LVESD, LVEF, and LVFS at 4 weeks after reperfusion. The data are expressed as the mean ± SE ($N = 8$ per group). The data were compared using one-way ANOVA followed by Bonferroni's multiple comparison test.

endogenous PPARγ induction in IR injury and cardiac healing/remodelling after MI. Nonetheless, PPARγ activation by exogenously administered pioglitazone-NPs exerted cardioprotective effects that were associated with NF-κB inhibition (*Figure 3B*), which was attributed to the PPARγ-dependent transrepression of NF-κB.[16,17]

In addition to inhibiting IR injury, pioglitazone-NPs attenuated cardiac remodelling in the mouse IR model (*Figure 5A* and *B*). According to the experimental protocol, we administered pioglitazone-NPs intravenously for three consecutive days, starting 6 h after LAD ligation, because inflammatory monocytes accumulate in the infarcted myocardium during the first few days after the onset of ischaemia and peak at 3 days after the onset of ischaemia.[41] Pioglitazone-NPs ameliorated increases in LVEDD and LVESD and decreases in LVEF and LVFS at 28 days after MI (Figure 6*C* and *D*, Supplementary material online, *Table S2*). Pioglitazone-NPs polarized macrophages toward a pro-healing M2 phenotype, increased TIMP1 expression, and inhibited MMP activity (*Figure 7C* and *E*), thus leading to cardiac dilatation attenuation and cardiac function improvement (Figure 6 C and *D*). We reasoned that increases in the M2 macrophage percentage would lead to excessive fibrosis; however, pioglitazone-NPs reduced Masson-trichrome-positive fibrosis areas at 28 days after LAD ligation (*Figure 6B*) because pioglitazone-NPs did not increase the total number of M2 macrophages and instead suppressed necrosis expansion by inhibiting excessive M1 macrophage-mediated inflammation. Furthermore, pioglitazone-NPs significantly decreased mortality rates by reducing cardiac rupture after MI (*Figure 6E* and *F*). The leading cause of mortality during the acute phase is cardiac rupture, which has been reported to be associated with extensive inflammation and the MMP response.[42–44] Pioglitazone-NPs increased TIMP1 expression, inhibited MMP activity, promoted scar formation, and prevented cardiac rupture. It is better to suppress inflammatory macrophages during the acute phase; however, pro-healing macrophages are necessary for cardiac healing during the repair phase as well. Therefore, the molecular pathways that balance inflammatory and pro-healing macrophage functions may be potential novel targets for therapeutic treatment after MI.

We demonstrated that pioglitazone-NPs decreased MCP-1 expression in primary cultured mouse cardiomyocytes (Supplementary material online, *Figure S8*). In a previous report,[45] inhibiting NF-κB nuclear translocation in cardiomyocytes decreased MCP-1 expression. This report, along with our results shown in *Figure 3B*, suggests that pioglitazone-NPs decreased MCP-1 expression in cardiomyocytes via the PPARγ-NF-κB pathway. In addition, it was previously reported that PPARγ agonists decrease apoptosis in cultured cardiomyocytes after hypoxia-reoxygenation.[46] These results suggest the direct effects of pioglitazone-NPs on cardiomyocytes. In contrast, pioglitazone-NPs inhibited THP-1 monocyte chemotaxis to MCP-1 (Supplementary material online, *Figure S10*), indicating that pioglitazone-NPs exerted direct effects on monocytes/macrophages. To elucidate the relative importance of monocytes/macrophages and other types of cells, including cardiomyocytes, as therapeutic targets of pioglitazone-NPs, we examined the effects of pioglitazone-NPs in $CCR2^{-/-}$ mice in which monocyte/macrophage recruitment to the heart was suppressed. In these mice, pioglitazone-NPs did not significantly decrease the infarct size. This finding suggests the primary role of CCR2+ monocytes as a therapeutic

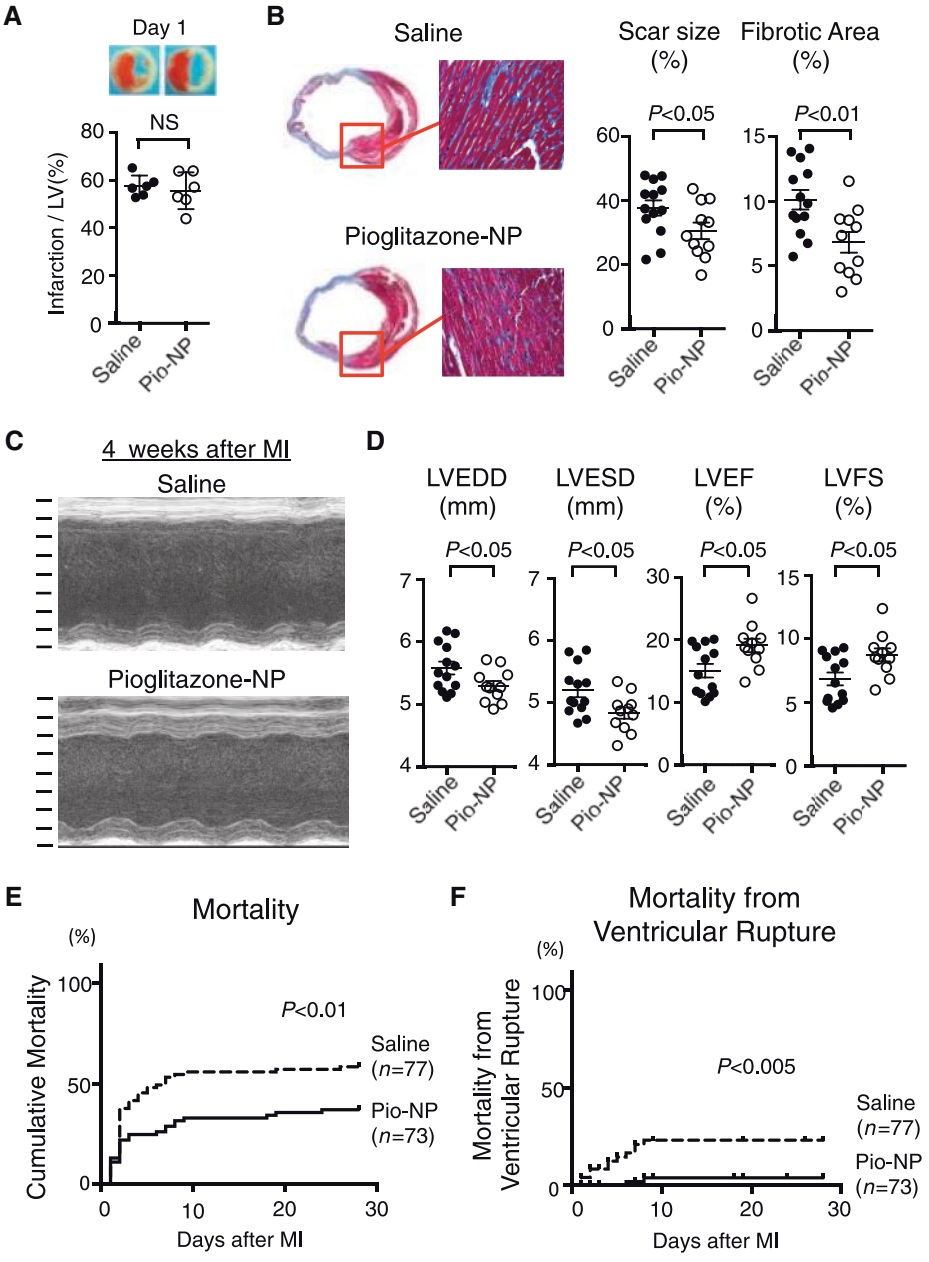

Figure 5 Pro-healing pioglitazone-NP effects in a mouse MI model. (*A*) Quantification of infarct size on Day 1. The data were compared using an unpaired *t*-test ($N = 6$ per group). NS, not significant. (*B*) Pioglitazone-NP effects on Masson-trichrome-positive scar area sizes and fibrosis in the border zone at 4 weeks after reperfusion. The data are expressed as the mean ± SE ($N = 13$: saline, $N = 11$: pioglitazone-NPs). The data were compared using an unpaired *t*-test. (*C*) Representative M-mode echocardiograms for animals treated with saline or pioglitazone-NPs at 4 weeks after LAD ligation. The interval of the scale is 1 mm. (*D*) Pioglitazone-NP effects on LVEDD, LVESD, LVEF, and LVFS at 4 weeks after reperfusion. The data are expressed as the mean ± SE ($N = 13$: saline, $N = 11$: pioglitazone-NPs). The data were compared using an unpaired *t*-test. (*E*) Kaplan–Meier survival analysis in mice treated with saline or pioglitazone-NPs after MI. $N = 77$: saline, $N = 73$: pioglitazone-NPs. (*F*) Mortality of MI mice due to ventricular rupture. $N = 77$: saline, $N = 73$: pioglitazone-NP.

target of pioglitazone-NPs. In addition, we have previously demonstrated that PLGA-NPs are delivered to endothelial cells.[23,26] Our data showing a reduction in ICAM1 expression after treatment with pioglitazone-NPs (*Table 1*) indicate the possibility that endothelial cells are also a therapeutic target of pioglitazone-NPs. Furthermore, pioglitazone-NPs resulted in approximately two-fold higher pioglitazone concentrations in the myocardium after ischaemia than did pioglitazone solution at a dose of 1 mg/kg; therefore, pioglitazone solution administered at a dose of 3.0 mg/kg was expected to have therapeutic effects. However, pioglitazone solution treatment showed no therapeutic effects, thus suggesting that (i) monocytes/macrophages rather than the myocardium after ischaemia were the primary target of pioglitazone-NPs or that (ii)

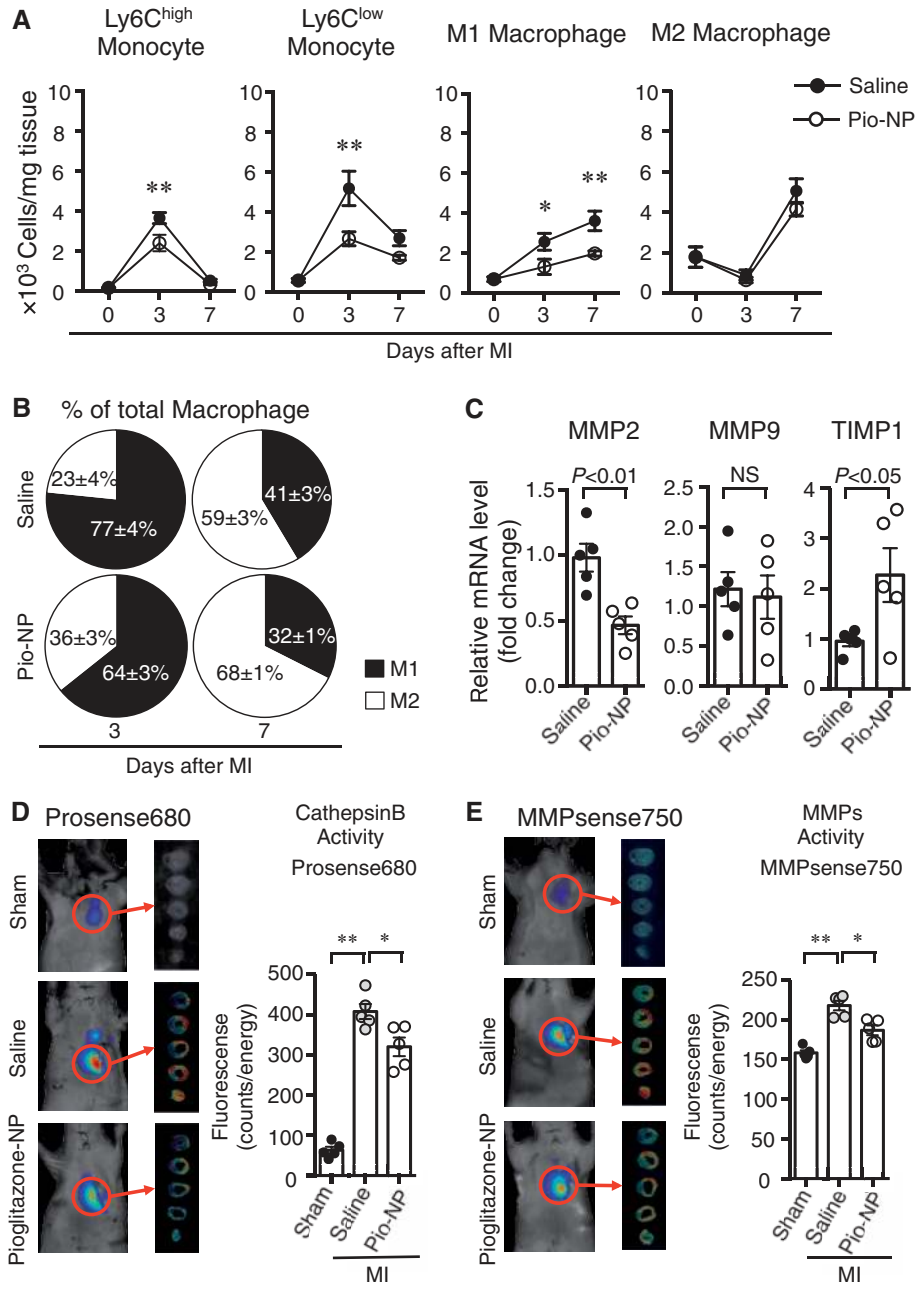

Figure 6 Pioglitazone-NP effects on myocardial remodelling and survival in a mouse MI model. (*A*) Flow cytometric analysis of the leucocytes in MI hearts treated with saline and pioglitazone-NPs. The data are expressed as the mean ± SE ($N = 6$ per group). *$P < 0.05$ and **$P < 0.01$ vs. the saline group using two-way ANOVA followed by Bonferroni's multiple comparison test. (*B*) Pioglitazone-NP effects on macrophage polarity. The data are expressed as the mean ± SE ($N = 6$ per group). (*C*) Pioglitazone-NP effects on MMP2, MMP9, and TIMP1 mRNA levels in the MI hearts. The data are expressed as the mean ± SE ($N = 5$ per group). The data were compared using an unpaired *t*-test. NS, not significant. (*D*, *E*) Coronal FMT image acquired 24 h after the injection of Prosense-680 and MMPsense-750. FRI imaging of sections of the heart 5 days after LAD ligation. Quantification of Prosense-680 and MMPsense-750 activation 5 days after LAD ligation. The data are reported as the mean ± SE ($N = 5$ per group). *$P < 0.01$ and **$P < 0.0001$ using one-way ANOVA followed by Bonferroni's multiple comparison test.

pioglitazone-NPs and the pioglitazone solution differ with respect to intracellular compartmentalization and thus differ in how they exert their anti-inflammatory effects.

With respect to its translation into a clinical setting, PLGA has a great advantage over other agents with respect to its safety profiles. PLGA is hydrolysed into lactic acid and glycolic acid and is then excreted from the body as CO_2 and H_2O via the Krebs cycle, causing minimal toxicity. PLGA is hydrolysed in saline for 21 days. The US FDA and European Medicine Agency (EMA) have approved PLGA for use in humans. PLGA NPs containing pitavastatin (an HMG-CoA reductase inhibitor)

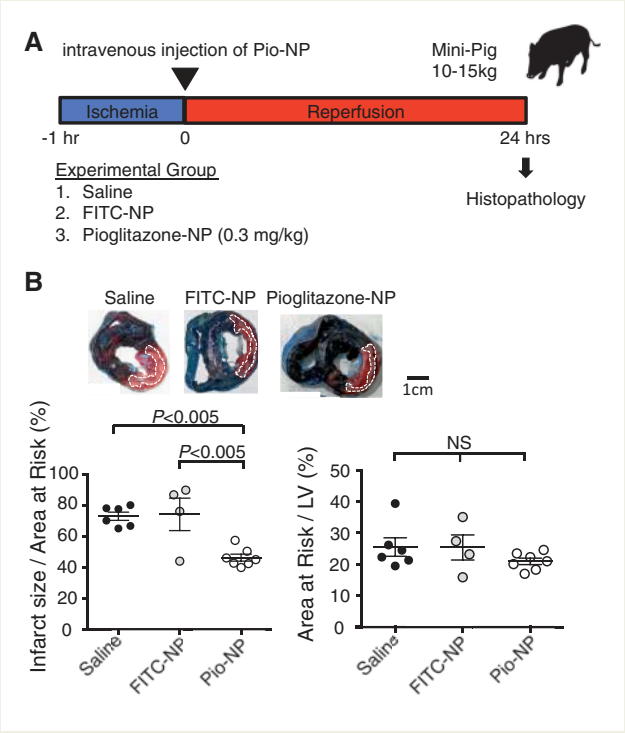

Figure 7 Therapeutic pioglitazone-NP effects on reperfused infarction in a porcine IR model. The effects of saline, FITC-NPs, and pioglitazone-NPs on infarct sizes after IR. The data are expressed as the mean ± SE ($N = 6$: saline, $N = 4$: FITC-NP, $N = 7$: pioglitazone-NP). The data were compared using one-way ANOVA followed by Bonferroni's multiple comparison test. NS, not significant.

produced by the same process have been investigated by the Japanese regulatory agency (Pharmaceuticals and Medical Devices Agency). We have started a Phase I/IIa investigative clinical trial at Kyushu University Hospital (clinical trial registry ID: UMIN000008011) and are investigating the efficacy of the PLGA NP-mediated delivery of pitavastatin in patients with critical limb ischaemia. Furthermore, the use of PPARγ agonists is hampered by their undesirable side effects, including oedema and heart failure, in clinical settings. However, there was no worsening of heart failure in mice administered pioglitazone-NPs. This may be because (i) pioglitazone-NPs were administered for 3 days when myocardial healing was occurring. (ii) In our previous study, the nanoparticulation of pioglitazone did not increase the expression levels of the epithelial Na^+ channel (ENaC), which is induced by PPARγ agonists and promotes the reabsorption of urine sodium in the kidney, thus suggesting that PLGA-NPs may cause fewer side effects than pioglitazone solution.[30]

In conclusion, pioglitazone-NPs protect the heart from IR injury and cardiac remodelling by antagonizing monocyte/macrophage-mediated acute inflammation and promoting cardiac healing after myocardial infarction. These effects are associated with M1/M2 macrophage polarity shifts in preclinical animal models. NP-mediated targeting of pioglitazone may be developed as a novel therapeutic modality with anti-inflammatory and pro-healing effects.

Supplementary material

Supplementary material is available at *Cardiovascular Research* online.

Acknowledgements

We thank Eiko Iwata and Satomi Abe for their excellent technical assistance.

Conflict of interest: K.E. holds a patent on the results reported in the present study. The remaining authors report no conflicts of interest. H.T. has received lecture fees (Astellas, Ohtsuka, Takeda, Daiichi-Sankyo, Tanabe-Mitsubishi, Boehringer-Ingelheim, Novartis, Bayer, and Bristol-Myers) and research funds (Daiichi-Sankyo, Astellas, and Actellion).

Funding

This study was supported by grants from the Ministry of Education, Science, and Culture, Tokyo, Japan (Grants-in-Aid for Scientific Research 25461135 to T.M. and 23790863 and 23790861 to K.E.); the Ministry of Health Labor and Welfare, Tokyo, Japan (Health Science Research Grants, Research on Translational Research, Intractable Diseases, and Nanomedicine to K.E.); and the Intractable Diseases Overcome Research Project from the Japan Agency for Medical Research and Development (AMED, to K.E.) and JST CREST Grant Number JPMJCR17H5, Japan.

References

1. Mozaffarian D, Benjamin EJ, Go AS, Arnett DK, Blaha MJ, Cushman M, Das SR, de Ferranti S, Després J-P, Fullerton HJ, Howard VJ, Huffman MD, Isasi CR, Jiménez MC, Judd SE, Kissela BM, Lichtman JH, Lisabeth LD, Liu S, Mackey RH, Magid DJ, McGuire DK, Mohler ER, Moy CS, Muntner P, Mussolino ME, Nasir K, Neumar RW, Nichol G, Palaniappan L, Pandey DK, Reeves MJ, Rodriguez CJ, Rosamond W, Sorlie PD, Stein J, Towfighi A, Turan TN, Virani SS, Woo D, Yeh RW, Turner MB. Heart disease and stroke statistics—2016 update. *Circulation* 2016;**133**:e38–e360.
2. Menees DS, Peterson ED, Wang Y, Curtis JP, Messenger JC, Rumsfeld JS, Gurm HS. Door-to-balloon time and mortality among patients undergoing primary PCI. *N Engl J Med* 2013;**369**:901–909.
3. Yellon DM, Hausenloy DJ. Myocardial reperfusion injury. *N Engl J Med* 2007;**357**:1121–1135.
4. Hausenloy DJ, Yellon DM. Myocardial ischemia-reperfusion injury: a neglected therapeutic target. *J Clin Invest* 2013;**123**:92–100.
5. Marchant DJ, Boyd JH, Lin DC, Granville DJ, Garmaroudi FS, McManus BM. Inflammation in myocardial diseases. *Circ Res* 2012;**110**:126–144.
6. Burchfield JS, Xie M, Hill JA. Pathological ventricular remodeling: mechanisms: part 1 of 2. *Circulation* 2013;**128**:388–400.
7. Faxon DP, Gibbons RJ, Chronos NAF, Gurbel PA, Sheehan F, Investigators H-M. The effect of blockade of the CD11/CD18 integrin receptor on infarct size in patients with acute myocardial infarction treated with direct angioplasty: the results of the HALT-MI study. *J Am Coll Cardiol* 2002;**40**:1199–1204.
8. Abbate A, Van Tassell BW, Biondi-Zoccai G, Kontos MC, Grizzard JD, Spillman DW, Oddi C, Roberts CS, Melchior RD, Mueller GH, Abouzaki NA, Rengel LR, Varma A, Gambill ML, Falcao RA, Voelkel NF, Dinarello CA, Vetrovec GW. Effects of interleukin-1 blockade with anakinra on adverse cardiac remodeling and heart failure after acute myocardial infarction [from the Virginia Commonwealth University-Anakinra Remodeling Trial (2) (VCU-ART2) Pilot Study]. *Am J Cardiol* 2013;**111**:1394–1400.
9. Liehn EA, Piccinini AM, Koenen RR, Soehnlein O, Adage T, Fatu R, Curaj A, Popescu A, Zernecke A, Kungl AJ, Weber C. A new monocyte chemotactic protein-1/chemokine CC motif ligand-2 competitor limiting neointima formation and myocardial ischemia/reperfusion injury in mice. *J Am Coll Cardiol* 2010;**56**:1847–1857.
10. Leuschner F, Dutta P, Gorbatov R, Novobrantseva TI, Donahoe JS, Courties G, Lee KM, Kim JI, Markmann JF, Marinelli B, Panizzi P, Lee WW, Iwamoto Y, Milstein S, Epstein-Barash H, Cantley W, Wong J, Cortez-Retamozo V, Newton A, Love K, Libby P, Pittet MJ, Swirski FK, Koteliansky V, Langer R, Anderson DG, Weissleder R, Nahrendorf M. Therapeutic siRNA silencing in inflammatory monocytes in mice. *Nat Biotechnol* 2011;**29**:1005–1010.
11. Nakano Y, Matoba T, Tokutome M, Funamoto D, Katsuki S, Ikeda G, Nagaoka K, Ishikita A, Nakano K, Koga J-I, Sunagawa K, Egashira K. Nanoparticle-mediated delivery of Irbesartan induces cardioprotection from myocardial ischemia-reperfusion injury by antagonizing monocyte-mediated inflammation. *Sci Rep* 2016;**6**:29601.
12. van Amerongen MJ, Harmsen MC, van Rooijen N, Petersen AH, van Luyn MJA. Macrophage depletion impairs wound healing and increases left ventricular remodeling after myocardial injury in mice. *Am J Pathol* 2007;**170**:818–829.
13. Ahmadian M, Suh JM, Hah N, Liddle C, Atkins AR, Downes M, Evans RM. PPARγ; signaling and metabolism: the good, the bad and the future. *Nat Med* 2013;**19**:557–566.

14. Libby P, Plutzky J. Inflammation in diabetes mellitus: role of peroxisome proliferator-activated receptor-α and peroxisome proliferator-activated receptor-γ agonists. *Am J Cardiol* 2007;**99**:27–40.
15. Brown JD, Plutzky J. Peroxisome proliferator activated receptors as transcriptional nodal points and therapeutic targets. *Circulation* 2007;**115**:518–533.
16. Ricote M, Glass CK. PPARs and molecular mechanisms of transrepression. *Biochim Biophys Acta* 2007;**1771**:926–935.
17. Abdelrahman M, Sivarajah A, Thiemermann C. Beneficial effects of PPAR-gamma ligands in ischemia-reperfusion injury, inflammation and shock. *Cardiovasc Res* 2005; **65**:772–781.
18. Bouhlel MA, Derudas B, Rigamonti E, Dièvart R, Brozek J, Haulon S, Zawadzki C, Jude B, Torpier G, Marx N, Staels B, Chinetti-Gbaguidi G. PPARγ activation primes human monocytes into alternative M2 macrophages with anti-inflammatory properties. *Cell Metab* 2007;**6**:137–143.
19. Odegaard JI, Ricardo-Gonzalez RR, Goforth MH, Morel CR, Subramanian V, Mukundan L, Eagle AR, Vats D, Brombacher F, Ferrante AW, Chawla A. Macrophage-specific PPARγ controls alternative activation and improves insulin resistance. *Nature* 2007;**447**:1116–1120.
20. Ricote M, Li AC, Willson TM, Kelly CJ, Glass CK. The peroxisome proliferator-activated receptor-gamma is a negative regulator of macrophage activation. *Nature* 1998;**391**:79–82.
21. Ye Y, Lin Y, Manickavasagam S, Perez-Polo JR, Tieu BC, Birnbaum Y. Pioglitazone protects the myocardium against ischemia-reperfusion injury in eNOS and iNOS knockout mice. *Am J Physiol Heart Circ Physiol* 2008;**295**:H2436–H2446.
22. Honda T, Kaikita K, Tsujita K, Hayasaki T, Matsukawa M, Fuchigami S, Sugiyama S, Sakashita N, Ogawa H, Takeya M. Pioglitazone, a peroxisome proliferator-activated receptor-γ agonist, attenuates myocardial ischemia–reperfusion injury in mice with metabolic disorders. *J Mol Cell Cardiol* 2008;**44**:915–926.
23. Kubo M, Egashira K, Inoue T, Koga JI, Oda S, Chen L, Nakano K, Matoba T, Kawashima Y, Hara K, Tsujimoto H, Sueishi K, Tominaga R, Sunagawa K. Therapeutic neovascularization by nanotechnology-mediated cell-selective delivery of pitavastatin into the vascular endothelium. *Arterioscler Thromb Vasc Biol* 2009;**29**:796–801.
24. Kimura S, Egashira K, Nakano K, Iwata E, Miyagawa M, Tsujimoto H, Hara K, Kawashima Y, Tominaga R, Sunagawa K. Local delivery of imatinib mesylate (STI571)-incorporated nanoparticle ex vivo suppresses vein graft neointima formation. *Circulation* 2008;**118**:S65–S70.
25. Chen L, Nakano K, Kimura S, Matoba T, Iwata E, Miyagawa M, Tsujimoto H, Nagaoka K, Kishimoto J, Sunagawa K, Egashira K. Nanoparticle-mediated delivery of pitavastatin into lungs ameliorates the development and induces regression of monocrotaline-induced pulmonary artery hypertension. *Hypertension* 2011;**57**:343–350.
26. Nagahama R, Matoba T, Nakano K, Kim-Mitsuyama S, Sunagawa K, Egashira K. Nanoparticle-mediated delivery of pioglitazone enhances therapeutic neovascularization in a murine model of hindlimb ischemia. *Arterioscler Thromb Vasc Biol* 2012;**32**: 2427–2434.
27. Katsuki S, Matoba T, Nakashiro S, Sato K, Koga JI, Nakano K, Nakano Y, Egusa S, Sunagawa K, Egashira K. Nanoparticle-mediated delivery of pitavastatin inhibits atherosclerotic plaque destabilization/rupture in mice by regulating the recruitment of inflammatory monocytes. *Circulation* 2014;**129**:896–906.
28. Nagaoka K, Matoba T, Mao Y, Nakano Y, Ikeda G, Egusa S, Tokutome M, Nagahama R, Nakano K, Sunagawa K, Egashira K. A new therapeutic modality for acute myocardial infarction: nanoparticle-mediated delivery of pitavastatin induces cardioprotection from ischemia-reperfusion injury via activation of PI3K/Akt pathway and anti-inflammation in a rat model. *PLoS One* 2015;**10**:e0132451.
29. Gustafson HH, Holt-Casper D, Grainger DW, Ghandehari H. Nanoparticle uptake: the phagocyte problem. *Nano Today* 2015;**10**:487–510.
30. Nakashiro S, Matoba T, Umezu R, Koga J-I, Tokutome M, Katsuki S, Nakano K, Sunagawa K, Egashira K. Pioglitazone-incorporated nanoparticles prevent plaque destabilization and rupture by regulating monocyte/macrophage differentiation in ApoE$^{-/-}$ mice. *Arterioscler Thromb Vasc Biol* 2016;**36**:491–500.
31. Kawashima Y, Yamamoto H, Takeuchi H, Hino T, Niwa T. Properties of a peptide containing dl-lactide/glycolide copolymer nanospheres prepared by novel emulsion solvent diffusion methods. *Eur J Pharm Biopharm* 1998;**45**:41–48.
32. Matsui Y, Takagi H, Qu X, Abdellatif M, Sakoda H, Asano T, Levine B, Sadoshima J. Distinct roles of autophagy in the heart during ischemia and reperfusion: roles of AMP-activated protein kinase and beclin 1 in mediating autophagy. *Circ Res* 2007;**100**: 914–922.
33. Hsu CP, Zhai P, Yamamoto T, Maejima Y, Matsushima S, Hariharan N, Shao D, Takagi H, Oka S, Sadoshima J. Silent information regulator 1 protects the heart from ischemia/reperfusion. *Circulation* 2010;**122**:2170–2182.
34. Ichimura K, Matoba T, Nakano K, Tokutome M, Honda K, Koga J-I, Egashira K. A translational study of a new therapeutic approach for acute myocardial infarction: nanoparticle-mediated delivery of pitavastatin into reperfused myocardium reduces ischemia-reperfusion injury in a preclinical porcine model. *PLoS One* 2016;**11**:e0162425.
35. Duan SZ, Usher MG, Mortensen RM. Peroxisome proliferator-activated receptor-γ-mediated effects in the vasculature. *Circ Res* 2008;**102**:283–294.
36. Kaikita K, Hayasaki T, Okuma T, Kuziel WA, Ogawa H, Takeya M. Targeted deletion of CC chemokine receptor 2 attenuates left ventricular remodeling after experimental myocardial infarction. *Am J Pathol* 2004;**165**:439–447.
37. Swirski FK, Nahrendorf M, Etzrodt M, Wildgruber M, Cortez-Retamozo V, Panizzi P, Figueiredo JL, Kohler RH, Chudnovskiy A, Waterman P, Aikawa E, Mempel TR, Libby P, Weissleder R, Pittet MJ. Identification of splenic reservoir monocytes and their deployment to inflammatory sites. *Science* 2009;**325**:612–616.
38. Mao Y, Koga J-I, Tokutome M, Matoba T, Ikeda G, Nakano K, Egashira K. Nanoparticle-mediated delivery of pitavastatin to monocytes/macrophages inhibits left ventricular remodeling after acute myocardial infarction by inhibiting monocyte-mediated inflammation. *Int Heart J* 2017;**58**:615–623.
39. Riva M, Källberg E, Björk P, Hancz D, Vogl T, Roth J, Ivars F, Leanderson T. Induction of nuclear factor-κB responses by the S100A9 protein is Toll-like receptor-4-dependent. *Immunology* 2012;**137**:172–182.
40. Fliegner D, Westermann D, Riad A, Schubert C, Becher E, Fielitz J, Tschöpe C, Regitz-Zagrosek V. Up-regulation of PPARγ in myocardial infarction. *Eur J Heart Fail* 2008;**10**:30–38.
41. Hilgendorf I, Gerhardt LMS, Tan TC, Winter C, Holderried TAW, Chousterman BG, Iwamoto Y, Liao R, Zirlik A, Scherer-Crosbie M, Hedrick CC, Libby P, Nahrendorf M, Weissleder R, Swirski FK. Ly-6Chigh monocytes depend on Nr4a1 to balance both inflammatory and reparative phases in the infarcted myocardium. *Circ Res* 2014; **114**:1611–1622.
42. Frangogiannis NG. Regulation of the inflammatory response in cardiac repair. *Circ Res* 2012;**110**:159–173.
43. Fang L, Gao X-M, Moore X-L, Kiriazis H, Su Y, Ming Z, Lim YL, Dart AM, Du X-J. Differences in inflammation, MMP activation and collagen damage account for gender difference in murine cardiac rupture following myocardial infarction. *J Mol Cell Cardiol* 2007;**43**:535–544.
44. Hayashidani S, Tsutsui H, Ikeuchi M, Shiomi T, Matsusaka H, Kubota T, Imanaka-Yoshida K, Itoh T, Takeshita A. Targeted deletion of MMP-2 attenuates early LV rupture and late remodeling after experimental myocardial infarction. *Am J Physiol Heart Circ Physiol* 2003;**285**:H1229–H1235.
45. Onai Y, Suzuki J, Kakuta T, Maejima Y, Haraguchi G, Fukasawa H, Muto S, Itai A, Isobe M. Inhibition of IκB phosphorylation in cardiomyocytes attenuates myocardial ischemia/reperfusion injury. *Cardiovasc Res* 2004;**63**:51–59.
46. Kilter H, Werner M, Roggia C, Reil J-C, Schäfers H-J, Kintscher U, Böhm M. The PPAR-gamma agonist rosiglitazone facilitates Akt rephosphorylation and inhibits apoptosis in cardiomyocytes during hypoxia/reoxygenation. *Diabetes Obes Metab* 2009; **11**:1060–1067.